Accepted Manuscript

Obestatin ameliorates water retention in chronic heart failure by downregulating renal aquaporin 2 through GPR39, V2R and PPARG signaling

Li-Zhi Bao, Ming Shen, Hannisa Qudirat, Jian-Bo Shi, Ting Su, Jing-Wen Song, Zhong-Kai Wang, Xian-Xian Zhao, Qing Jing, Xing Zheng, Zhi-Fu Guo

Obestatin ameliorates water retention in chronic heart failure by downregulating renal aquaporin 2 through GPR39, V2R and PPARG signaling

Li-Zhi Bao [a], Ming Shen [a], Hannisa Qudirat [a], Jian-Bo Shi [b], Ting Su [a], Jing-Wen Song [a], Zhong-Kai Wang [a], Xian-Xian Zhao [a], Qing Jing [a,*], Xing Zheng [a,*], and Zhi-Fu Guo [a,*]

[a] Department of Cardiology, Changhai Hospital, Naval Medical University, Shanghai, 200433, China; chdocsmmu@163.com (L.-Z.B.); yeyue0725@163.com (M.S.); m13319031873@163.com (H.Q.); st.hy.kn@163.com (T.S.); qingniao_SJW@163.com (J.-W.S.); 13816038626@163.com (Z.-K.W.); zhaoxianxian168@126.com (X.-X.Z.)

[b] Department of Cardiology, HongKou Branch of Changhai Hospital of PLA, Shanghai, 200081, China; stevenshi12@126.com (J.-B. S.)

[*] Correspondence: qjing@sibs.ac.cn, (86-21)31161266 (Q.J.); zhengxing57530@163.com, (86-21)31161246 (X.Z.); guozhifu@126.com, (86-21)31161263 (Z.-F.G.)

The first three authors contributed equally to this study.

A B S T R A C T

Aims: Obestatin regulates water metabolism by inhibiting arginine vasopressin (AVP) release and upregulated obestatin has been detected in patients with chronic heart failure (CHF). However, the significance of obestatin in CHF, particularly with regard to water retention and aquaporin 2 (AQP2) expression, remains unknown.

Main methods: Using a CHF rat model, the effects of 2-week exogenous obestatin administration were evaluated. Expression of AQP2 was evaluated by immunoblotting, immunohistochemical staining, and quantitative real-time PCR (qPCR) in CHF rat model and mouse inner medullary collecting duct (mIMCD) 3 cell line. Moreover, the influence of obestatin on the genetic transcription profile in mIMCD3 cells was evaluated by microarray, and the potential regulatory mechanisms of obestatin on AQP2 were evaluated by RNA silencing of vasopressin receptor 2 (V2R), peroxisome proliferator-activated receptor gamma (PPARG), and G protein-coupled receptor 39 (GPR39).

Key findings: Obestatin increased urinary output and improved expression of CHF biomarker without significantly altering cardiac function, plasma electrolyte concentrations, or the plasma AVP concentration. AQP2 expression was significantly reduced. The results of microarray analyses and qPCR indicated that mRNA levels of *Aqp2*, *Pparg*, and *V2r* were significantly decreased. Inhibition of *V2r* and *Pparg* mRNA further reduced the expression of AQP2, while the inhibitory efficacy of obestatin on AQP2 was significantly offset after *Gpr39* knockdown.

Significance: Long-term treatment with obestatin improves water retention in CHF by increasing urinary output through downregulation of AQP2 expression in renal IMCD cells. These effects may be at least partially mediated by regulation of GPR39, V2R and PPARG signaling.

Keywords: Obestatin; Aquaporin2; GPR39; Heart failure; Collecting duct

1. Introduction

Chronic heart failure (CHF) is a severe clinical syndrome that occurs in the end stage of various cardiovascular diseases. Water retention is an important pathophysiological characteristic of CHF and contributes to a variety of clinical symptoms, such as breathlessness and edema. Typically, diuretics are used to relieve these symptoms through increased urinary output. However, long-term use of conventional diuretics may expose patients to metabolic disorders and electrolyte imbalance [1-3]. Therefore, development of a novel treatment against water retention that does not significantly influence the electrolyte balance is important for improving the treatment of CHF patients.

The aquaporin (AQP) family consists of transmembrane proteins that function via the transport channel for water and other small molecule solutes, and 13 AQPs have been identified in mammals to date [4, 5]. Among them, aquaporin 2 (AQP2), which is located in the luminal plasma membrane and intracellular vesicles in the principle cells of renal collecting ducts (CDs), has been recognized as the key regulator of water reabsorption and urine concentration, likely via regulation of the water permeability of CDs [6]. It has been confirmed that upregulated AQP2 in the luminal plasma membrane and the associated increase in water reabsorption are the most important pathophysiological mechanisms for water retention in patients with CHF [7]. In fact, novel diuretics targeting AQP2, such as tolvaptan, have been shown to be promising for patients with diseases related to water retention, including CHF [8, 9].

Obestatin is a 23-amino acid polypeptide homologous to ghrelin that has been suggested to exert various biological functions via activation by amidation [10]. Previous studies confirmed that the physiological function of obestatin may include regulation of appetite, body weight, lipid metabolism, and vascular endothelial functions [11-13]. Interestingly, a previous study showed that intracerebroventricular injection of obestatin may regulate water metabolism by acting on the thirst center [14]. More importantly, obestatin reduced renal reabsorption of water by inhibiting arginine vasopressin (AVP)-mediated expression and activation of AQP2 [14]. Moreover, the results of our previous research showed that the level of obestatin in the peripheral circulation was significantly higher in patients with CHF than in healthy controls [15]. Since plasma obestatin is unable to enter the thirst center through the blood–brain barrier and its receptor GPR39 is abundantly expressed in kidney, we hypothesized that the upregulated obestatin in CHF may regulate water metabolism by acting on the renal system. Therefore, in this study, we evaluated the potential influence of exogenous obestatin on water retention and AQP2 expression in the renal CDs. Moreover, the potential mechanisms underlying the regulatory effects of obestatin on AQP2 expression were explored via microarray analysis and gene silencing technique.

2. Materials and Methods

2.1. Main materials

The mouse inner medullary CD (mIMCD) 3 cell line was purchased from JENNIO Biotech (Guangzhou, China). Obestatin and NA-obestain (nonamidated obestatin), were synthetized by GL Biochem (Shanghai, China). Desmopressin (dDAVP) and obestatin anti-serum (obestatin-IgG, 1 mg/ml) were purchased from Phoenix Pharmaceuticals (Burlingame, CA). Mozavaptan (OPC-31260, OPC) was purchased from Selleckchem (Houston, TX, USA). The lentiviral pLKO.1 plasmid vector was kindly shared by the Shanghai institute for Biological Sciences.

2.2. Animal experiments

Pathogen-free male Sprague–Dawley rats (7 weeks old, body weight 180~200 g) were provided by Shanghai SIPPR-BK Laboratory Animal Co. Ltd. [Animal license number: SCXK (Shanghai) 2013-0016]. The rats were weighed every week, fed commercial rat chow, given free access to water, and housed under a 12-h light/12-h dark cycle at a temperature of 25 ± 2°C. All experimental protocols, which were in agreement with laboratory animal management and use regulations, had been approved by the Animal Care and Use Committee of Second Military Medical University before the performance of the study. All rats were acclimatized for 5 days before modeling. CHF was induced by myocardial infarction (MI) via ligation of the left anterior descending branch (LAD) of the coronary artery [16]. For the rats assigned to the sham group, the same procedure was performed without ligation of the LAD. Limb lead electrocardiograms (ECGs) were recorded during the whole process to evaluate the effect of ligation. MI model rats were fed normally for 6 weeks. Then according to transthoracic echocardiography results (Table 1), the surviving rats were screened by the criterion of an ejection fraction (EF) value ≤45% [17, 18] as the successful CHF model. The selected CHF model rats were randomly assigned to the following seven groups (n=6 rats per group) according to different treatments (intravenously injected twice daily in 200 µl physiological saline): blank model group (labeled CHF, physiological saline), high-dose obestatin group (labeled ob-H, 200 µg/kg body weight, BW), low-dose obestatin group (labeled ob-L, 100 µg/kg BW) [19], NA-obestatin group (labeled NA, 200 µg/kg BW), dDAVP group (labeled dDAVP, 2 µg/kg BW) [20], OPC-31260 group (labeled OPC, 1 mg/rat) [21], obestatin-IgG group (labeled ob-IgG, 3 µg/rat) [14]. Along with the rats in the sham group (labeled sham, *n*=6) which were given physiological saline similarly, rats in a total of eight groups were treated for 2 weeks. Among the above groups, the CHF and NA groups served as negative control groups, and the OPC31260 (a selective vasopressin receptor 2 [V2R] antagonist) and dDAVP (agonist to V2R) groups served as positive control groups representing the downregulating and upregulating effects on renal AQP2, respectively.

Table 1. Ejection Fraction of groups at the 6th week after MI modeling operation

Groups（n=6）	LVEF(%)
sham	73.11±3.45
CHF	37.50±3.69***
NA	37.89±3.62***
Ob-H	36.16±6.03***
Ob-L	37.05±4.79***
OPC	36.99±4.33***
dDAVP	37.76±3.00***
ob-IgG	37.28±4.47***

The data are presented as the means ± SD. *** denotes P < 0.001, compared with sham group. LVEF, left ventricular ejection fraction.

2.3. Transthoracic echocardiography measurements

Transthoracic echocardiography was performed in anesthetized rats to evaluate the morphology, ventricular wall motion, and function of the left ventricle using an iU22 color Doppler ultrasound diagnostic instrument and S5-1 high frequency probe (Philips, Boston, MA, USA). Parameters obtained included left ventricular internal diameter at end-systole (LVIDs), left ventricular internal diameter at end-diastole (LVIDd), left ventricular end-diastolic volume (LVDV), and left ventricular end-systolic volume (LVSV), of which the latter two were calculated by bullet equation [22]. The left

ventricular ejection fraction (LVEF) and shortening fraction (LVFS) were calculated by Simpson method [23]. Three cardiac cycles were continuously measured, and the data obtained were averaged for further analysis.

2.4. Collection and processing of urine and plasma samples

Twenty-four–hour urine samples were collected before and after the treatments by placing all rats in individual metabolic cages. At the same time, total volumes of 24-h urine samples were recorded and adjusted for body weight. Serum samples of 1ml were collected in duplicate from the femoral vein at 6th and 8th week after anesthesia using heparin lithium anticoagulant tubes and EDTA-K2 anticoagulant tubes. After collection, plasma samples were centrifuged (4°C, 3000 g/min, 10 min). The medium yellow clear liquid was transferred to a new tube and stored at -80°C until assay performance. The plasma in heparin lithium tubes was used for electrolyte detection, and that in EDTA-K2 tubes was used for brain-type natriuretic peptide (BNP), AVP, and obestatin measurements. Electrolyte levels in plasma samples were measured by a HITACH 7600 Biochemical Analyzer (Hitachi, Tokyo, Japan) automatically according to the manufacturer's instructions. Plasma BNP, AVP, and obestatin levels were measured using enzyme-linked immunosorbent assay (ELISA) kits (Westang, Shanghai, China). The sensitivity limits of the assays were 16 pg/mL, 10 pg/mL, and 14 pg/ml, respectively.

2.5. Preparation of kidney tissue for RNA and protein extraction

At the end of week 8, all rats were anesthetized and euthanized. Kidney samples were rapidly harvested and rinsed with cold physiological saline. The inner medulla was dissected from the right kidney and divided into two parts. One half was ground in TRIzol Reagent (Invitrogen, CA, USA) for RNA isolation using a glass homogenizer on ice, and the other half was ground in radio immunoprecipitation assay (RIPA) Lysis Buffer containing 0.1 M phenylmethylsulfonyl fluoride (PMSF) for protein extraction.

2.6. Preparation of kidney tissue for immunohistochemical staining

The left kidneys of rats were perfused and fixed in 4% neutral paraformaldehyde for 24 h before dehydration with a gradient of ethanol concentrations. Dehydrated samples were embedded in paraffin wax and then 5-μm paraffin sections were prepared for immunohistochemical examination. Briefly, endogenous peroxidase was blocked in 3% H_2O_2 for 10 min at room temperature. For antigen retrieval, sections were heated in a microwave oven and then boiled in a mixed retrieval solution (1 mM Tris, pH 9.9 with 0.5 mM EDTA) for 10 min. After cooling naturally, the sections were blocked in phosphate-buffered saline (PBS) containing 3% bovine serum albumin (BSA) and then incubated with AQP2 antibody (1:200 dilution) in PBS with 0.1% BSA and 0.3% Triton X-100 at 4°C overnight. After three 5-min washes with PBS, sections were incubated with horseradish peroxidase-conjugated secondary antibody at room temperature for 60 min. Upon rinsing with PBS buffer, the regions of antibody–antigen reaction were visualized with DAB (3-diaminobenzidine) color-substrate solution. Brown stained regions were the target protein-positive areas. Moreover, the nuclei were visualized by hematoxylin staining. Photographs of the stained sections were taken under microscopy (Leica, Wetzlar, Germany) with the same optical parameters. Six different regions in each section were analyzed twice. Protein expression was assessed through the mean density acquired from areas of interest analyzed by Image-Pro plus 6.0 (Media Cybernetics, MD, USA). Two researchers performed the evaluation independently. The mean density was calculated based on the following formula: mean density = integrated optical density (IOD)/area.

2.7. mIMCD3 cell culture and treatments

Cells were cultured in a 1:1 mixture of Dulbecco's Modified Eagle's Medium and Ham's F12 medium (DMEM/F12) supplemented with 10% fetal bovine serum (Gibco, ThermoFisher, MA, USA) in a humidified incubator with a 5% CO_2 atmosphere at 37°C. Once the mIMCD3 cells reached approximately 70% confluency, the medium was replaced with serum-free DMEM/F12 medium for 12

h. After serum starvation, the cells were treated with obestatin of different concentrations or for different durations to determine the optimal treatment regimen. Once the optimal conditions for obestatin stimulation were determined, the cells were divided into seven groups treated with PBS (Con group), obestatin-IgG (10 μg/ml) for 1 hour prior to obestatin (10^{-7} mM, ob + ob-IgG group), dDAVP (10^{-7} mM, dDAVP group), NA-obestatin (10^{-7} mM, NA group), obestatin (10^{-7} mM, ob-H group), obestatin (0.5×10^{-7} mM, ob-L group), and OPC31260 (10^{-7} mM, OPC group).

2.8. RNA extraction and qPCR analysis

Interventionary studies involving animals or humans, and other studies require ethical approval must list the authority that provided approval and the corresponding ethical approval code.

Total RNA was extracted from approximately 50 mg renal inner medullary tissue or 4×10^5 mIMCD3 cells using TRIzol Reagent. The concentrations and quality of total RNA were measured at an optical density ratio of 260/280 using the Nanodrop ND-1000 spectrophotometer. The integrity of the total RNA obtained was verified on an Agilent 2100 Bioanalyzer using the RNA 6000 Nano LabChip (Agilent, CA, USA). One microgram of total RNA from each sample was decontaminated of genomic DNA and then reverse transcribed to cDNA using the PrimeScript RT reagent Kit with gDNA Eraser (Takara Bio, Otsu, Japan). qPCR was used to evaluate the mRNA expression of the different genes of interest, and performed in a mixture comprising 10 μl SYBR Master Mix (Toyobo, Osaka, Japan), 0.4 μl forward primer and 0.4 μl reverse primer for the corresponding gene, 7.2 μl of nuclease-free water, and 2 μl of cDNA sample diluted 1:10, for a final volume of 20 μl. B-Actin was used as an endogenous control gene. All cDNA samples were amplified through a Rotor-Gene RG-3000A instrument (Corbett Research, Sydney, Australia) according to the following steps: 1 cycle of 95°C for 10 s, 40 cycles of 95°C for 5 s, 58–62°C for 10 s (optimized for each primer pair), and 72°C for 15 s. The melt curve was completed at the end of the last cycle when the temperature was increased from 60 to 98°C. The primers used for qPCR (Table A1 and A2) were synthesized by Sangon Biotech (Shanghai, China). Relative quantification of different gene expression levels was achieved using the $2^{-\triangle\triangle CT}$ formula and data from three independent experiments [24].

2.9. Immunoblotting analysis

Protein was extracted from approximately 50 mg renal inner medullary tissue or 4×10^5 mIMCD3 cells using RIPA Lysis Buffer along with 0.1 M PMSF. The concentrations of protein were measured using a BCA test kit (Beyotime Biotech., Haimen, China). Equal amounts (50 μg) of protein from different groups were separated by 10% sodium dodecyl sulfate polyacrylamide gel electrophoresis (SDS-PAGE) and transferred onto polyvinylidene difluoride membranes, which were then incubated with primary antibodies at 4°C overnight. The following rabbit polyclonal antibodies were used: anti-AQP2 (1:2000, Abcam, Cambridge, UK), anti-V2R (1:500, Biorbyt, Cambridge, UK), anti-PPARG (1:1000, Abcam, Cambridge, UK), anti-B-ACTIN (1:2000, Servicebio, Wuhan, China), and anti-GPR39 (1:500, Novus, Colorado, USA). The membranes were further incubated with horseradish peroxidase-conjugated anti-rabbit IgG (1:2000, Cell Signaling, MA, USA) for 2 h at room temperature. Enhanced chemiluminescent visualization was performed, and the ImageQuant LAS 4000 Gel Imaging System (GE Healthcare, Uppsala, Sweden) was used to capture the luminous protein bands. Three samples in each group were used for protein extraction, and the experiments were performed in triplicate. Image J software (NIH image, Bethesda, MD, USA) was used for image analysis.

2.10. Microarray analysis and qPCR verification

Interventionary studies involving animals or humans, and other studies require ethical approval must list the authority that provided approval and the corresponding ethical approval code.

After serum starvation, mIMCD3 cells at about 80% confluency were divided into two groups (n=3 samples per group), which were treated with obestatin (10^{-7} mM) or PBS for 24 h. Then total RNA was extracted using the TRIzol method and verified for concentration, purity, and integrity as described above. One half of the RNA samples were reverse transcribed into cDNA and stored at −80°C until

further qPCR verification, and the other half of the same batch were applied to the following microarray test (GeneChip Mouse Genome 430 2.0 Array, Affymetrix, CA, USA) according to the manufacturer's instructions. Finally, the images and the original data were obtained through scanning with the GeneChip Scanner 3000 (Affymetrix, CA, USA) and decoding with GeneAtlas software. A more in-depth analysis was carried out via a bioinformatics study. The selected genes of interest were further verified by qPCR.

2.11. shRNA silencing of gene expression

A puromycin-resistant lentiviral pLKO.1 plasmid vector was used for RNA silencing. First, the nucleotide sequences of the *V2r*, *Pparg*, and *Gpr39* mRNAs were obtained in GENEBANK database. Two corresponding short hairpin RNA (shRNA) interference target sequences for each gene (Table 2) were selected using the siRNA selection tool (Ambion website, TX, USA). Then, they were cloned into the linearized pLKO.1 plasmid vector, which was achieved by AgeI and EcoR1 restriction site cutting to construct the pLKO.1-*V2r*-shRNA, pLKO.1-*Pparg*-shRNA, and pLKO.1-*Gpr39*-shRNA recombinant plasmids. After connection, transformation, and sequencing identification, mIMCD3 cells were transfected with the recombinant plasmids using Lipofectamine 2000 (Invitrogen, CA, USA). The pLKO.1-control-shRNA plasmid with a scrambled sequence was used as the control. Cells successfully transfected with the pLKO.1 plasmids were selected with 5 μg/ml puromycin (Merck, Darmstadt, Germany), and stable clones were maintained in 2.5 μg/ml puromycin. Then the silencing efficiencies of the three genes above were determined by qPCR. One of the most efficient silencing clones was selected for each gene, and the constructed mIMCD3 cell lines with stable interference were stored at -80°C for further research.

Table 2. Sequences of shRNAs from muttus *V2r*, *Pparg* and *Gpr39* cDNA

NO.	5'	STEMP	Loop	STEMP	3'
shRNA-V2r 1# F:	CCGGTC	GCATGCCCATGGAGTTCTACA	TTCAAGAGA	TGTAGAACTCCATGGGCATGC	TTTTTTgg
shRNA-V2r 1# R:	AATTCCCAAAAAA	GCATGCCCATGGAGTTCTACA	TCTCTTGAA	TGTAGAACTCCATGGGCATGC	GA
shRNA-V2r 2# F:△	CCGGTC	GCATGCCAACCAAGAGAAACG	TTCAAGAGA	CGTTTCTCTTGGTTGGCATGC	TTTTTTgg
shRNA-V2r 2# R:△	AATTCCCAAAAAA	GCATGCCAACCAAGAGAAACG	TCTCTTGAA	CGTTTCTCTTGGTTGGCATGC	GA
shRNA-Pparg 1# F:	CCGGTC	GGATGTCTCACAATGCCATCA	TTCAAGAGA	TGATGGCATTGTGAGACATCC	TTTTTTgg
shRNA-Pparg 1# R:	AATTCCCAAAAAA	GGATGTCTCACAATGCCATCA	TCTCTTGAA	TGATGGCATTGTGAGACATCC	GA
shRNA-Pparg 2# F:△	CCGGTC	GCAAGAGATCACAGAGTATGC	TTCAAGAGA	GCATACTCTGTGATCTCTTGC	TTTTTTgg
shRNA-Pparg 2# R:△	AATTCCCAAAAAA	GCAAGAGATCACAGAGTATGC	TCTCTTGAA	GCATACTCTGTGATCTCTTGC	GA
shRNA-Gpr39 1# F:	CCGGTC	GCATGCCCATGGAGTTCTACA	TTCAAGAGA	TGTAGAACTCCATGGGCATGC	TTTTTTgg
shRNA-Gpr39 1# R:	AATTCCCAAAAAA	GCATGCCCATGGAGTTCTACA	TCTCTTGAA	TGTAGAACTCCATGGGCATGC	GA
shRNA-Gpr39 2# F:△	CCGGTC	GCATGCCAACCAAGAGAAACG	TTCAAGAGA	CGTTTCTCTTGGTTGGCATGC	TTTTTTgg
shRNA-Gpr39 2# R:△	AATTCCCAAAAAA	GCATGCCAACCAAGAGAAACG	TCTCTTGAA	CGTTTCTCTTGGTTGGCATGC	GA

# indicates the different sequence of the same gene. △ indicates the finally selected shRNA sequence according to the silencing efficiency.

2.12. Statistical analysis

All experimental data are presented as mean ± standard deviation (SD) and were analyzed with the statistical software SPSS 20.0 (SPSS Inc, Chicago, IL, USA). Differences between groups or within groups were analyzed by single factor analysis of variance (ANOVA) with Bonferroni testing. For comparisons between only two groups, the independent t-test was utilized. $P<0.05$ was considered statistically significant.

3. Results

3.1. Plasma obestatin level was increased in CHF rat models

To confirm the previous findings in humans with CHF [15], we evaluated the plasma concentration of obestatin in the peripheral circulation of rats with MI-induced CHF at 6 weeks after operation by ELISA. The results showed that the plasma obestatin level was significantly greater in the CHF group compared with the sham group (1923±59.29 pg/ml vs. 1601±44.22 pg/ml, P<0.01, Figure 1A).

3.2. Obestatin increased urinary output and improved HF biomarkers without influencing cardiac function or plasma electrolyte levels

Urinary output was markedly increased after treatment with high-dose or low-dose obestatin for 2 weeks (75.18±8.51, 63.69±8.91 vs. 40.77±5.49, 41.37±6.56 ml/kg BW, respectively, Figure 1B). In addition, in the ob-H or ob-L groups, plasma BNP level, which was regarded as a biomarker related to the diagnosis and progression of HF [25, 26], were significantly lower than those in the CHF group (1152.61±99.31, 1223.75±95.17 vs. 1504.54±85.62 pg/ml, Figure 1C). In addition, the NA group showed no differences compared with the CHF group. Obestatin-IgG showed reverse effects compared with obestatin treatment. However, the cardiac structure and function indexes as well as electrolyte concentrations in plasma did not differ significantly among all seven modeling groups (Table 3 and 4). Altogether, these results indicate that obestatin has a dose-dependent diuretic effect that may lead to improvement of CHF.
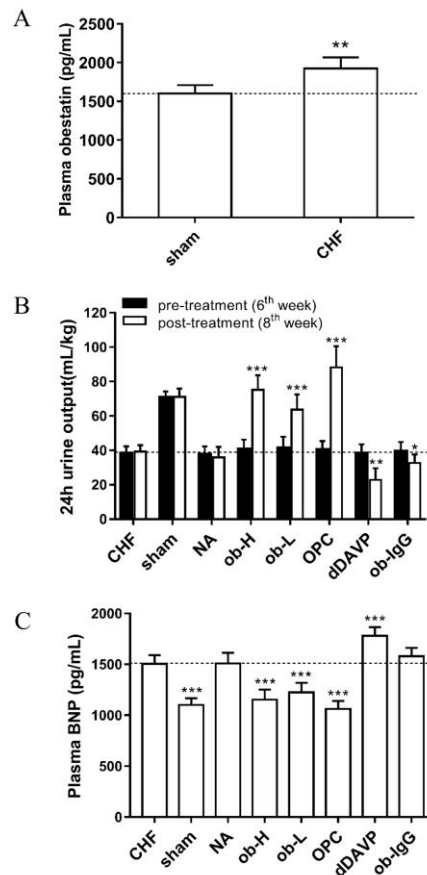

Figure 1. Plasma level of obestatin and its potential effect on urinary volume and biomarker of CHF in rat models. Groups treated with physiological saline, physiological saline and sham surgery, NA-obestatin (200 μg/kg), obestatin (200 μg/kg), obestatin (100 μg/kg), OPC31260 (1 mg), dDAVP (2 μg/kg), obestatin-IgG (3 μg) were labeled as CHF, sham, NA, ob-H, ob-L, OPC, dDAVP, and ob-IgG, respectively. (A) Comparison of peripheral plasma levels of obestatin in the CHF group and sham group before treatment (n=6). **P<0.01. (B) Urinary output was significantly increased in the rats treated with high-dose or low-dose obestatin. *P<0.05, **P<0.01, and ***P<0.001 compared with pre-treatment values. (C) Plasma BNP was decreased in the rats treated with obestatin at the 8th week compared with the level in the CHF group. ***P<0.001. Data are presented as the means ± SD.

Table 3. Echocardiographic parameters in sham-operated rats and rats with heart failure after receiving different treatments (8th week, n=6).

Groups	LVIDd（mm）	LVIDs（mm）	LVDV（μl）	LVSV（μl）	LVEF%	LVFS%
CHF	8.95±1.06	7.27±0.92	448.56±121.77	282.70±83.31	37.25±3.56	18.87±1.99
sham	6.47±0.80***	3.71±0.50***	217.10±60.36**	60.02±19.00***	72.30±4.24***	42.49±3.98***
NA	8.82±0.30	7.16±0.29	428.55±32.27	269.15±24.35	37.23±1.97	18.84±1.12
ob-H	9.48±0.73	7.76±0.86	504.76±87.81	326.28±83.84	36.03±5.34	18.28±2.96
ob-L	9.30±0.87	7.64±0.82	485.24±103.09	314.67±79.88	35.44±3.76	17.89±2.09
OPC	8.88±0.76	7.13±0.62	437.88±85.04	268.39±52.31	38.65±4.38	19.70±2.52
dDAVP	9.16±0.54	7.50±0.54	466.56±62.14	300.32±49.90	35.80±3.06	18.08±1.71
ob-IgG	8.98±0.39	7.30±0.54	446.66±43.30	282.22±49.37	37.12±2.07	18.83±2.81

The data are presented as the means ± SD. **, *** denotes P < 0.01 and P < 0.001 compared with other modeling groups.

Table 4. Plasma electrolyte concentrations in sham-operated rats and rats with heart failure after receiving different treatments (8th week, n=6).

Groups	Plasma concentrations(mmol/L)		
	sodium	potassium	chloride
CHF	144.50±1.87	5.13±0.23	100.00±2.53
sham	143.83±1.72	5.05±0.19	101.50±1.05
NA	144.17±1.94	4.98±0.25	99.33±1.86
ob-H	144.00±1.10	5.05±0.38	100.83±0.98
ob-L	142.50±0.84	5.17±0.28	101.00±2.00
OPC	144.33±1.63	4.87±0.23	99.00±2.90
dDAVP	143.33±2.73	5.10±0.36	99.67±3.72
ob-IgG	144.67±1.63	5.03±1.97	101.17±4.67

The data are presented as the means ± SD

3.3. Obestatin decreased AQP2 expression in renal inner medullary tissue but had no effect on the plasma AVP level

Immunohistochemical examination suggested that AQP2 protein abundance in the inner medulla was significantly higher than that of the outer medulla and the cortex (IOD value 6229.9±994.3, 4069.7±586.8, 825.6±172.4, respectively) in CHF rats, and mostly decreased after high dose obestatin treatment (IOD value 2303.1±467.1, 1528.6±561.3, 351.4±329.8, decent degree 63.0%, 62.4%, 57.4%, in IMCD, OMCD, CCD respectively, Figure 2A). Thus, we focus on the inner medulla in the different groups with the techniques of qPCR, immunohistochemical straining, and immunoblotting to address whether AQP2 signaling is responsible for the increased urine output after obestatin treatment. As shown in Figure 2B, *Aqp2* mRNA expression was significantly lower in the ob-H and ob-L groups than in the CHF group (0.46±0.04 fold and 0.64±0.11 fold changes, respectively). In contrast, *Aqp2* mRNA expression was higher in the ob-IgG group than in the CHF group (1.19±0.07 fold change), suggesting ob-IgG could neutralize endogenous obestatin, thereby attenuating its effects on Aqp2 expression. Consistently, the results of immunohistochemical staining and immunoblotting analyses showed similar differences among the different groups (Figure 2C and 2D). AQP2 expression in the upregulated positive control group (dDAVP group) and downregulated positive control group (OPC group) also revealed corresponding changes as expected. Moreover, immunohistochemical staining showed localized expression of labeled AQP2 protein specifically in the IMCDs.

AVP, a potent circulating hormone, is closely related with water retention in CHF. In our study, the plasma AVP level in the CHF group was significantly elevated compared with that in the sham

group (12.13±0.74 pg/ml vs. 8.75±0.84 pg/ml)(Figure 2E). However, the plasma AVP level was not significantly altered by obestatin treatment in either the ob-H or ob-L group. These results suggest that obestatin has no influence on the plasma AVP level.
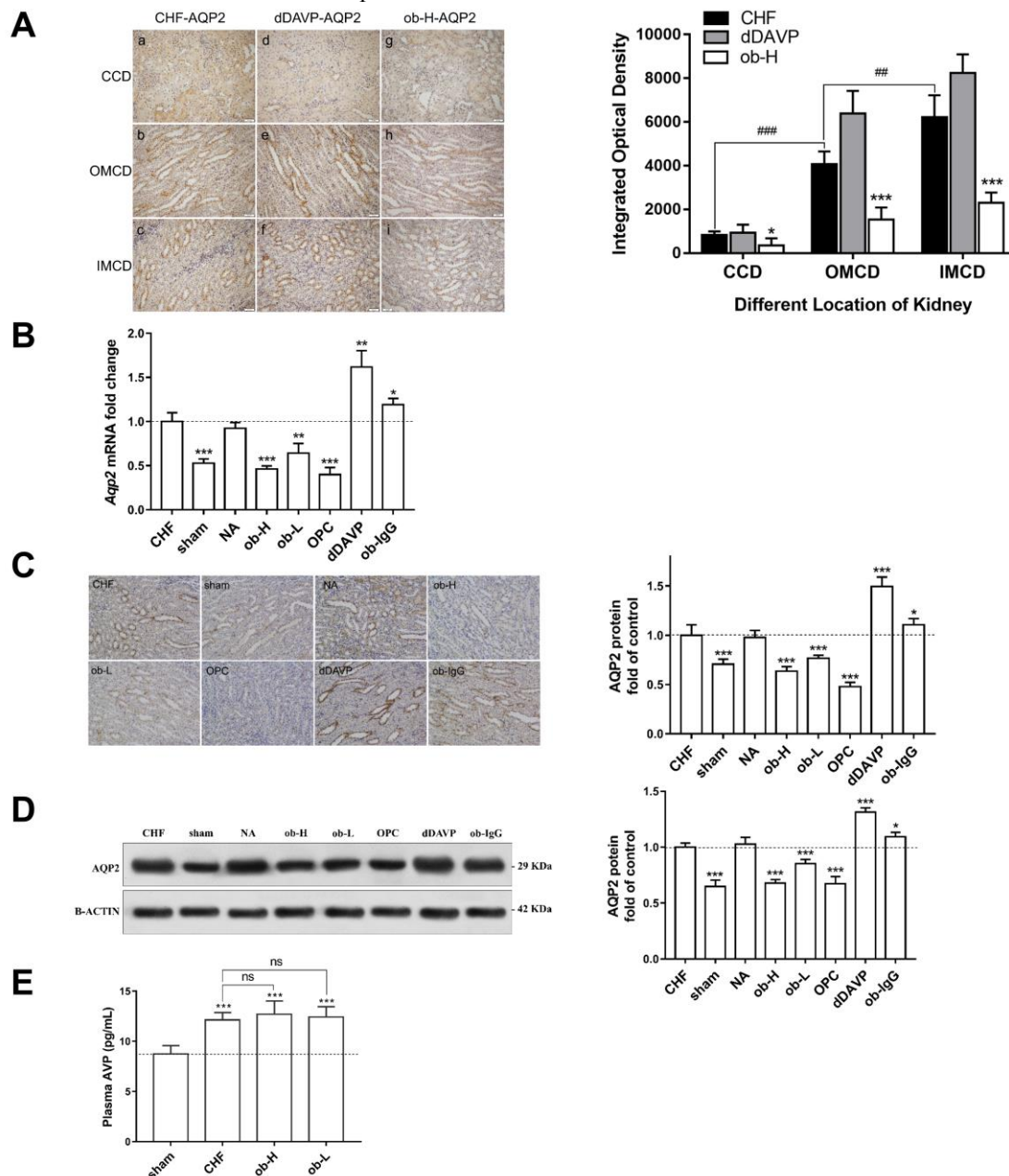

Figure 2. Chronic effects of obestatin on AQP2 expression in renal collect duct tissue and AVP level in plasma. (A) Immunohistochemical examination of AQP2 protein abundance in the renal CCD, OMCD, IMCD in a tissue section from rats of CHF group (a-c), dDAVP group (d-f) and ob-H group (g-i). Brown staining indicates AQP2 protein expression in the collecting ducts, and blue staining indicates cell nuclei. The AQP2 expression of the inner medulla was significantly higher than that of the outer medulla and the cortex, and decreased mostly after obestatin treatment. Scale bar 50μm, Magnification 200×. (B) Changes in *Aqp2* mRNA expression in renal inner medulla tissue after 2 weeks of treatment. (C) Immunohistochemical staining for AQP2 expression in different groups at a magnification of 200×. AQP2 expression was much stronger in the dDAVP and ob-IgG groups than in the CHF group; in contrast, labeling was much weaker in the sham, ob-H, ob-L, and OPC groups. Densitometric analysis data normalized by CHF group are shown in the bar graph. (D) Immunoblotting of AQP2 protein in the renal inner medulla post-treatment for different groups. Mean data for band densities of AQP2 protein normalized by B-ACTIN are shown in the bar graph. *P<0.05, **P<0.01, and ***P<0.001 above compared with the CHF group. ## and ### above, means P<0.01 and P<0.001. (E) Plasma AVP was elevated in

CHF modeling rats, but not influenced by obestatin treatment for 2 weeks. ***P<0.001 compared with the sham group. ns, not significant. The data above are presented as the means ± SD.

3.4. Obestatin decreases AQP2 expression in mIMCD3 cell line

In order to establish the optimal concentration for obestatin treatment, we treated mIMCD3 cells with four different concentration gradients of obestatin and observed the abundance of AQP2 protein via immunoblotting. We found that 10^{-7} mM obestatin decreased AQP2 protein expression more remarkably than the other three concentrations (by 43±3% vs. PBS, Figure 3A).

Furthermore, mIMCD3 cells were stimulated with obestatin for different time durations, and *Aqp2* gene expression was determined by qPCR. We found that at 6, 12, 24, 36, and 48 h of treatment with 10^{-7} mM obestatin, *Aqp2* expression was significantly decreased compared with that in the control group (0 h). In the range of 6 to 24 h, the downward trend with time was more remarkable, but after 36 h, the downregulated *Aqp2* mRNA expression gradually rebounded. Consistently, immunoblotting of AQP2 protein revealed a similar trend with increasing duration of 10^{-7} mM obestatin treatment (Figure 3B).

On the other hand, *Aqp2* gene expression was determined by qPCR at 24 h after different interventions. Compared with that in the Con group, the expression levels of the *Aqp2* gene in the ob-H, ob-L, and OPC groups were significantly decreased by 49±8%, 26±9%, and 56±8%, respectively. In contrast, the levels of *Aqp2* gene expression in the ob+ob-IgG and dDAVP group were increased by 11±6% and 93±11%, respectively; however, the difference between the ob+ob-IgG group and the Con group was not statistically significant (P>0.05). The *Aqp2* expression in the NA group did not differ statistically from that in the Con group. Compared with that in the ob-H group, *Aqp2* expression in the ob+ob-IgG group increased significantly from 51±8% to 111±6%, indicating that the effect of obestatin on *Aqp2* could be counteracted by ob-IgG.

These changes in *Aqp2* gene expression in mIMCD3 cells exposed to different treatments were further confirmed by the results of immunoblotting for AQP2 protein (Figure 3C).
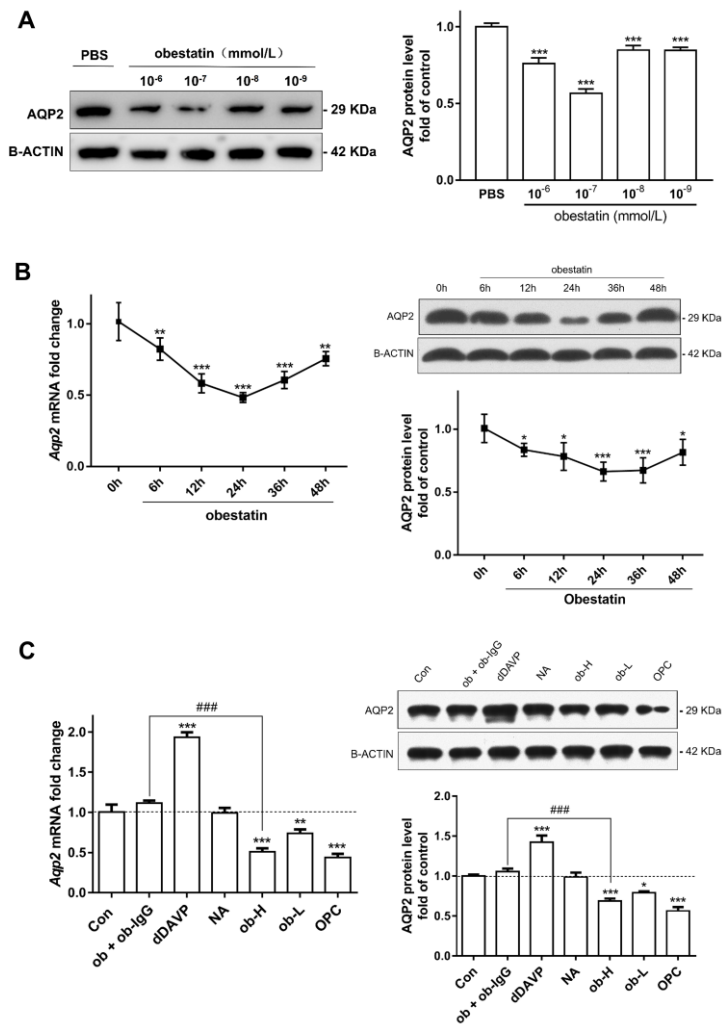
Figure 3. Obestatin decreased AQP2 expression in the mIMCD3 cell line. (A) Immunoblotting of AQP2 protein in mIMCD3 cells stimulated with obestatin at different concentrations (10^{-6}, 10^{-7}, 10^{-8}, or 10^{-9} mM) for 24 h. Mean data for band densities of AQP2 protein normalized by B-ACTIN are shown in the bar graph. (B) The mIMCD3 cells were stimulated with obestatin (10^{-7} mM) for 6, 12, 24, 36, or 48 h. Changes in AQP2 mRNA and protein expression were observed by qPCR or Immunoblotting. Mean data for AQP2 expression normalized by B-ACTIN were showned in the bar graph. (C) The mIMCD3 cells were subjected to different treatments as follows: PBS, obestatin (10^{-7} mM) plus obestatin-IgG (10 μg/ml), dDAVP (10^{-7} mM), NA-obestatin (10^{-7} mM), obestatin (10^{-7} mM), obestatin (0.5×10^{-7} mM), or OPC31260 (10^{-7} mM), and the groups were labeled Con, ob+ob-IgG, dDAVP, NA, ob-H, ob-L, and OPC, respectively. Changes in AQP2 mRNA and protein expression were observed by qPCR or Immunoblotting. Mean data for AQP2 expression normalized by B-ACTIN were showned in the bar graph. The data are presented as the means ± SD. *$P<0.05$, **$P<0.01$, and ***$P<0.001$ compared with the Con (0 h or PBS) group. ###$P<0.001$ as compared with the ob-H group.

3.5. Screening for differentially expressed genes via microarray analysis and validation of these by qPCR in the mIMCD3 cell line

To identify potential action targets for long-term obestatin function, we assessed the changes in the expression of three pairs of mRNAs in mIMCD3 cell line samples through gene chip screening. The cells were treated with obestatin (10^{-7} mM) or PBS for 24 h. Then the potential changes in the genetic transcription profiles in response to obestatin treatment were analyzed using GeneAtlas. Clustering analysis was used to visualize the differential expression in comparison to the PBS control (Figure 4). The results showed that obestatin treatment resulted in the differential expression of 1260 genes. Six hundred nine among them were downregulated, and 651 were upregulated (Figure 5A). Seventy-three genes were selected for further validation by qPCR, which included the 69 most differentially expressed genes (60 genes downregulated and 9 upregulated), 3 genes related

to renal water metabolism (*Aqp1*, *Aqp3*, and *Aqp4*), and the other gene *Gpr39*, which was previously linked to the function of obestatin[27] (Figure 5B).

As shown in Figure 5C, the qPCR results confirmed that obestatin treatment decreased the mRNA levels of *Pparg*, *Aqp2*, and *V2r* by 0.46±0.07, 0.63±0.06, 0.75±0.05 fold, respectively (all P<0.01). Unlike the downregulated genes, the upregulated genes detected by microarray showed no significant change upon qPCR validation, as did *Gpr39* and the other three genes.
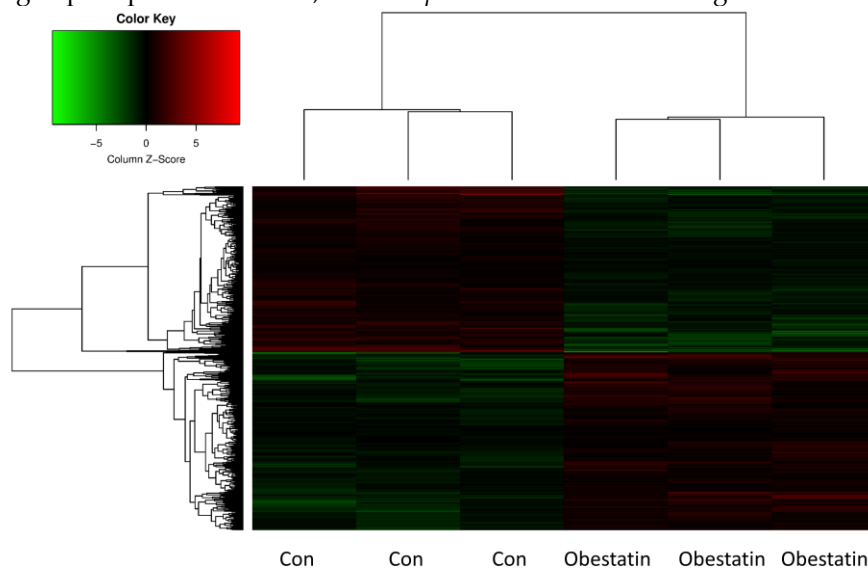

Figure 4. Cluster diagram of the differentially expressed genes in mIMCD3 cells after treatment with obestatin compared with PBS control.
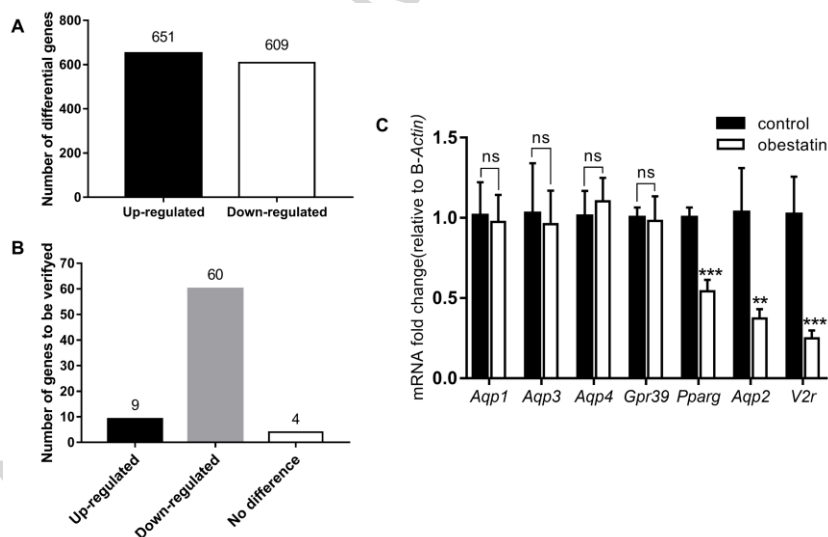

Figure 5. Major genes of interest identified as differentially regulated upon obestatin treatment using microarray analysis and validation by qPCR. (A) All differentially expressed genes revealed by microarray with a confidence level of P<0.05. (B) Selected genes of interest to be verified. Nine upregulated genes and 60 downregulated genes were found to be most differentially expressed by microarray. Among the four genes showing no difference, three (*Aqp1*, *Aqp3*, and *Aqp4*) were related to renal water metabolism, and the other gene (*Gpr39*) was considered as a possible receptor of obestatin. (C) Validation of results by qPCR. The data are presented as the means ± SD. **P<0.01 and ***P<0.001.

3.6. Effects of obestatin on AQP2, V2R, PPARG, and GPR39 expression after shRNA interference

First, the efficiency of shRNA on the *V2r*, *Pparg*, and *Gpr39* genes was evaluated by qPCR. Under these conditions, the constructs reduced *V2r* expression by 42±5%, *Pparg* expression by

44±7%, and *Gpr39* expression by 57±5% (Figure 6A, B). Second, as shown in Figure 6A and 6B, the silencing of *V2r* and *Pparg* together with obestatin treatment decreased the gene expression of *V2r*, *Pparg*, and *Aqp2* to a more remarkable extent than the reductions observed after any single intervention. However, no effects of obestatin on *Gpr39* gene expression with or without the silencing of *Gpr39* were observed, and the silencing of *Gpr39* weakened the effects of obestatin on *Aqp2* gene expression as compared with the results from the shRNA control group (62±6% in the shRNA control group vs. 91±9% in the shRNA *Gpr39* group).

Third, immunoblotting confirmed the effects of obestatin on AQP2 protein expression in cells with *V2r*, *Pparg*, or *Gpr39* knockdown. The results revealed changes consistent with the results of our qPCR analysis discussed above(Figure 6C).

Taken together, these results suggest that obestatin downregulated AQP2 expression through the inhibition of V2R and PPARG, which could be regarded as the downstream target of obestatin. Moreover, GPR39 may play a key role in obestatin function.
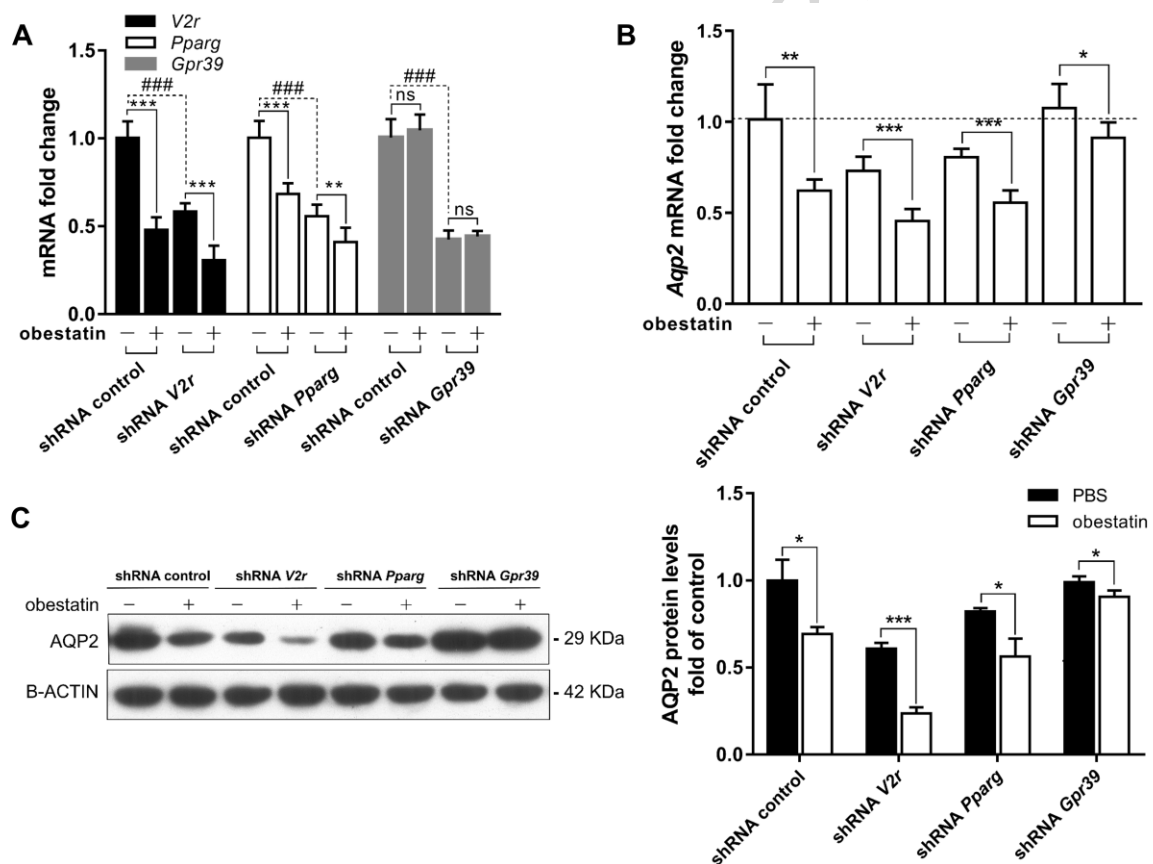

Figure 6. Effects of obestatin on the expression of AQP2, V2R, PPARG, and GPR39 after shRNA interference. (A) Efficiency of shRNA acting on *V2r*, *Pparg*, and *Gpr39* genes. (B) Changes in *Aqp2* mRNA expression level after shRNA interference of *V2r*, *Pparg*, and *Gpr39* expression. (C) Immunoblotting of AQP2 protein after shRNA interference of *V2r*, *Pparg*, and *Gpr39* expression. Mean data for band densities of proteins normalized by B-ACTIN are shown in the bar graph. The data above are presented as the means ± SD. *P<0.05, **P<0.01, and ***P<0.001. ###P<0.001. ns, not significant.

3.7. Obestatin exerts its effects on V2R and PPARG through GPR39 in mIMCD3 cells

The silencing of GPR39 could potently weaken the effects of obestatin on AQP2 expression, but whether it can influence V2R and PPARG expression remains unknown. Therefore, we evaluated the expression levels of V2R and PPARG proteins under the condition of GPR39 knockdown.

We prepared a stably GPR39-deficient mIMCD3 cell line as described above. The effect of GPR39 knockdown on V2R and PPARG expression was evaluated with or without obestatin

treatment. The results of immunoblotting revealed that GPR39 knockdown reversed the obestatin-activated decreases in V2R and PPARG protein expression from 44 ± 2% and 71 ± 4% to 87 ± 4% and 92 ± 2%, respectively, observed after treatment with obestatin (10^{-7} mM, 24 h, Figure 7). These results indicate that obestatin exerts its inhibitory effects on V2R and PPARG protein expression through GPR39.
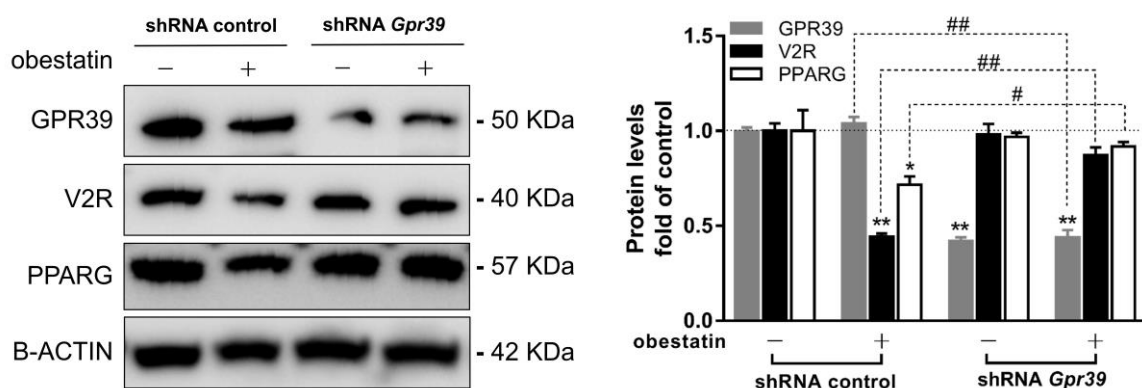

Figure 7. Effect of *Gpr39* knockdown by shRNA on the expression levels of V2R and PPARG in mIMCD3 cells. The mIMCD3 cells were transfected with shRNA *Gpr39* and subcultured for stable knockdown prior to obestatin treatment (10^{-7} mM, 24 h). The abundances of V2R, PPARG, and GPR39 proteins were denoted as fold change relative to the levels in the shRNA control group. The protein expression was normalized relative to B-ACTIN expression. The data are presented as the means ± SD. **P<0.01 as compared with the shRNA control group not treated with obestatin. #P<0.05 and ##P<0.01.

4. Discussion

In this study, we found that increased obestatin in peripheral circulation of CHF may be an important feature of CHF. Moreover, long-term treatment with exogenous obestatin was associated with increased urinary volume without a significant effect on the electrolyte concentration in plasma, along with significantly decreased expression of the biomarker of CHF. Subsequent studies showed that the benefits of obestatin for diuresis in CHF may be dependent on the interaction of GPR39 and inhibition of V2R and PPARG pathways, which finally lead to the downregulation of renal AQP2 expression. These results suggest that long-term treatment with obestatin improves water retention in CHF by increasing urinary output via downregulation of AQP2 expression in renal IMCDs. These effects may be at least partially mediated by regulation of GPR39, V2R, and PPARG signaling.

Previous studies have confirmed that the regulation of AQP2 is both AVP dependent and independent. The AVP-dependent mechanism [28-30] mainly involves the upregulation of AQP2 expression and enhanced AQP2 phosphorylation resulting from increased release of AVP from the supraoptic and paraventricular nucleus in the hypothalamus [31]. This mechanism responds to the increased plasma osmotic pressure, and increased AVP binds to V2R on the basolateral membrane of principle cells and triggers the classical cAMP-PKA pathway to induce increased water reabsorption via regulation of AQP2. On the other hand, the AVP-independent mechanism [28, 29, 32] mainly involves other factors involved in the regulation of AQP2 in addition to AVP. Previous studies showed that calcitonin activates its receptor and then activates adenylyl cyclase through a pathway similar to the post-AVP signaling pathway. Otherwise, PPARG, a type II nuclear receptor in the kidney that is mainly located in the principal cells of IMCDs[33, 34], has a close relationship with the renal water metabolism, and recent research has shown that activation of PPARG by GI262570 or Rosiglitazone increases Aqp2 mRNA expression, which finally accelerates the transfer of AQP2 vesicles to the luminal membrane, thereby increasing water reabsorption [35, 36]. PPARG knockout mice develop a polyuria phenotype without variation in urinary AVP excretion, suggesting PPARG

may play a role in directly regulating AQP2 expression apart from the AVP/V2R/cAMP/PKA pathway [37, 38]. Even so, the regulatory effect of PPARG on AQP2 remains controversial [39].

In this study, in vivo and in vitro experiments confirmed that obestatin downregulated the expression of AQP2 in the IMCDs of kidney, and the diuretic effect and the improvement of biochemical index of HF was also observed in vivo. However, there were no significant changes in the EF value and heart structure indexes, suggesting that obestain had little effect on myocardial remodeling. Moreover, no changes in peripheral blood AVP were observed after obestatin treatment, suggesting that the regulation of AQP2 by obestatin occurred independently from the classical AVP-dependent pathway. Bioinformatic analysis of the microarray data and validation by qPCR showed that obestatin downregulated *Aqp2* gene expression through two signaling pathways: *V2r* and *Pparg*. No variation was observed in the expression of additional genes related to renal water metabolism, such as *Aqp1*, *Aqp3*, and *Aqp4*.

Since its discovery in 2005, the reported biological functions of obestatin have varied from a role as a gastrointestinal-central endocrine hormone peptide during development to a systemic multi-organism regulatory peptide. The beneficial effects of obestatin on the cardiovascular system have attracted increasing attention [13, 40, 41], but studies on the regulation of renal water metabolism and the underlying mechanism are rare. Earlier studies once considered that GPR39 is the only exclusive receptor of obestatin *in vivo* [42], but subsequent studies have raised more controversy [43, 44]. However, the receptor of obestain in these clinical circumstances remains to be determined.

In this study, we focused on the effect of long-term obestatin treatment on the expression of AQP2 in renal inner medulla through a rat model of CHF and the mIMCD3 cell line. We also explored the possible mechanisms using a high-throughput microarray technique. According to the validated differentially expressed genes, we constructed shRNA vectors that interfered with the expression of three key genes for *V2r*, *Pparg*, and *Gpr39* and observed the subsequent regulatory effects of obestatin on AQP2 expression.

The degree of AQP2 protein downregulation was more remarkable after V2R and *Pparg* mRNA interference, but the inhibitory effects of AQP2, V2R, and PPARG induced with obestatin treatment were significantly attenuated after *Grp39* knockdown. These results suggest that GPR39 was the upstream target of obestatin through which obestatin may downregulate the expression of AQP2 protein via V2R and PPARG dual-pathway. Furthermore, obestatin has no regulatory effect on GPR39 itself, which suggests that GPR39 may partly serve as the receptor of obestatin, although this "receptor" role is controversial because of uncertain specificity [45]. Because it has been proven that V2R and GPR39 are both located on the cell membrane, the mechanism of their interaction warrants further investigation.

5. Conclusions

The elevated level of plasma obestatin in CHF may have a beneficial compensatory effect, just like the character of BNP. Long-term treatment with obestatin improves water retention in CHF by increasing urinary output via the downregulation of AQP2 expression in renal IMCDs. These effects may be at least partially mediated by regulation of GPR39, V2R, and PPARG signaling. Central and peripheral obestatin play a similar role in regulating water metabolism. Obestatin may be a novel effective diuretic target for CHF that is similarly to V2R antagonists worthy of further study.

Abbreviations: AVP: arginine vasopressin; CHF: chronic heart failure; AQP: aquaporin; qPCR: quantitative real-time PCR; mIMCD: mouse inner medullary collecting duct; GPR39: G protein-coupled receptor 39; CDs: collecting ducts; dDAVP: desmopressin; MI: myocardial infarction; LAD: left anterior descending branch; ECG: electrocardiogram; EF: ejection fraction; BW: body weight; V2R: vasopressin receptor 2; LVIDs: left ventricular internal diameter at end-systole; LVIDd: left ventricular internal diameter at end-diastole; LVDV: left ventricular end-diastolic volume; LVSV: left ventricular end-systolic volume; LVEF: left ventricular ejection fraction; LVFS: left ventricular shortening fraction; BNP: brain-type natriuretic peptide; RIPA: radio immunoprecipitation assay; PMSF: phenylmethylsulfonyl fluoride; PBS: phosphate-buffered saline; BSA: bovine serum albumin; IOD: integrated optical density; DMEM: Dulbecco's Modified Eagle's Medium; shRNA: short hairpin RNA; PPARG: peroxisome proliferator-activated receptor gamma.

References

[1] Savage PJ, Pressel SL, Curb JD, Schron EB, Applegate WB, Black HR, Cohen J, Davis BR, Frost P, Smith W, et al. Influence of long-term, low-dose, diuretic-based, antihypertensive therapy on glucose, lipid, uric acid, and potassium levels in older men and women with isolated systolic hypertension: The Systolic Hypertension in the Elderly Program. SHEP Cooperative Research Group, Arch Intern Med. 158 (1998) 741-751.

[2] Carter BL, Einhorn PT, Brands M, He J, Cutler JA, Whelton PK, Bakris GL, Brancati FL, Cushman WC, Oparil S, et al. Thiazide-induced dysglycemia: call for research from a working group from the national heart, lung, and blood institute, Hypertension. 52 (2008) 30-36.

[3] Gupta S, Neyses L. Diuretic usage in heart failure: a continuing conundrum in 2005, Eur Heart J. 26 (2005) 644-649.

[4] Fujiyoshi Y, Mitsuoka K, de Groot BL, Philippsen A, Grubmuller H, Agre P, Engel A. Structure and function of water channels, Curr Opin Struct Biol. 12 (2002) 509-515.

[5] Rojek A, Praetorius J, Frokiaer J, Nielsen S, Fenton RA. A current view of the mammalian aquaglyceroporins, Annu Rev Physiol. 70 (2008) 301-327.

[6] Kwon TH, Frøkiær J, Nielsen S. Regulation of aquaporin-2 in the kidney: A molecular mechanism of body-water homeostasis, Kidney Research & Clinical Practice. 32 (2013) 96.

[7] Bae EH, Ma SK. Water and sodium regulation in heart failure, Electrolyte Blood Press. 7 (2009) 38-41.

[8] Konstam MA, Kiernan M, Chandler A, Dhingra R, Mody FV, Eisen H, Haught WH, Wagoner L, Gupta D, Patten R, et al. Short-Term Effects of Tolvaptan in Patients With Acute Heart Failure and Volume Overload, J Am Coll Cardiol. 69 (2017) 1409-1419.

[9] Inomata T, Ikeda Y, Kida K, Shibagaki Y, Sato N, Kumagai Y, Shinagawa H, Ako J, Izumi T. Effects of Additive Tolvaptan vs. Increased Furosemide on Heart Failure With Diuretic Resistance and Renal Impairment- Results From the K-STAR Study, Circ J. 82 (2017) 159-167.

[10] Zhang JV, Ren PG, Avsian-Kretchmer O, Luo CW, Rauch R, Klein C, Hsueh AJ. Obestatin, a peptide encoded by the ghrelin gene, opposes ghrelin's effects on food intake, Science. 310 (2005) 996-999.

[11] Agnew AJ, Robinson E, McVicar CM, Harvey AP, Ali IH, Lindsay JE, McDonald DM, Green BD, Grieve DJ. The gastrointestinal peptide obestatin induces vascular relaxation via specific activation of endothelium-dependent NO signalling, Br J Pharmacol. 166 (2012) 327-338.

[12] Schinzari F, Veneziani A, Mores N, Barini A, Di Daniele N, Cardillo C, Tesauro M. Vascular Effects of Obestatin in Lean and Obese Subjects, Diabetes. 66 (2017) 1214-1221.

[13] Cowan E, Burch KJ, Green BD, Grieve DJ. Obestatin as a key regulator of metabolism and cardiovascular function with emerging therapeutic potential for diabetes, Br J Pharmacol. 173 (2016) 2165-2181.

[14] Samson WK, Yosten GL, Chang JK, Ferguson AV, White MM. Obestatin inhibits vasopressin secretion: evidence for a physiological action in the control of fluid homeostasis, J Endocrinol. 196 (2008) 559-564.

[15] Shi JB, Guo ZF, Zheng X, Wang ZB, Ma YJ. Circulating obestatin is increased in patients with cardiorenal syndrome and positively correlated with vasopressin, Peptides. 38 (2012) 377-380.

[16] Selye H, Bajusz E, Grasso S, Mendell P. Simple techniques for the surgical occlusion of coronary vessels in the rat, Angiology. 11 (1960) 398-407.

[17] Wang XF, Qu XQ, Zhang TT, Zhang JF. Testosterone suppresses ventricular remodeling and improves left ventricular function in rats following myocardial infarction, Exp Ther Med. 9 (2015) 1283-1291.

[18] Zhang L, Gan ZK, Han LN, Wang H, Bai J, Tan GJ, Li XX, Xu YP, Zhou Y, Gong ML, et al. Protective effect of heme oxygenase-1 on Wistar rats with heart failure through the inhibition of inflammation and amelioration of intestinal microcirculation, J Geriatr Cardiol. 12 (2015) 353-365.

[19] Koc M, Kumral ZN, Ozkan N, Memi G, Kacar O, Bilsel S, Cetinel S, Yegen BC. Obestatin improves ischemia/reperfusion-induced renal injury in rats via its antioxidant and anti-apoptotic effects: role of the nitric oxide, Peptides. 60 (2014) 23-31.

[20] Guron G, Nilsson A, Nitescu N, Nielsen S, Sundelin B, Frokiaer J, Friberg P. Mechanisms of impaired urinary concentrating ability in adult rats treated neonatally with enalapril, Acta Physiol Scand. 165 (1999) 103-112.

[21] Christensen BM, Marples D, Jensen UB, Frokiaer J, Sheikh-Hamad D, Knepper M, Nielsen S. Acute effects of vasopressin V2-receptor antagonist on kidney AQP2 expression and subcellular distribution, Am J Physiol. 275 (1998) F285-297.

[22] Wyatt HL, Meerbaum S, Heng MK, Gueret P, Corday E. Cross-sectional echocardiography. III. Analysis of mathematic models for quantifying volume of symmetric and asymmetric left ventricles, Am Heart J. 100 (1980) 821-828.

[23] Wasmeier GH, Melnychenko I, Voigt JU, Zimmermann WH, Eschenhagen T, Schineis N, Reulbach U, Flachskampf FA, Daniel WG, Nixdorff U. Reproducibility of transthoracic echocardiography in small animals using clinical equipment, Coron Artery Dis. 18 (2007) 283-291.

[24] Schmittgen TD, Livak KJ. Analyzing real-time PCR data by the comparative C(T) method, Nat Protoc. 3 (2008) 1101-1108.

[25] Ishikawa S. Urinary excretion of aquaporin-2 in pathological states of water metabolism, Ann Med. 32 (2000) 90-93.

[26] Gaggin HK, Januzzi JL, Jr. Biomarkers and diagnostics in heart failure, Biochim Biophys Acta. 1832 (2013) 2442-2450.

[27] Moechars D, Depoortere I, Moreaux B, De SB, Goris I, Hoskens L, Daneels G, Kass S, Ver DL, Peeters T. Altered gastrointestinal and metabolic function in the GPR39-obestatin receptor-knockout mouse, Gastroenterology. 131 (2006) 1131.

[28] Fenton RA, Pedersen CN, Moeller HB. New insights into regulated aquaporin-2 function, Curr Opin Nephrol Hypertens. 22 (2013) 551-558.

[29] Tamma G, Procino G, Svelto M, Valenti G. Cell culture models and animal models for studying the patho-physiological role of renal aquaporins, Cell Mol Life Sci. 69 (2012) 1931-1946.

[30] Wilson JL, Miranda CA, Knepper MA. Vasopressin and the regulation of aquaporin-2, Clin Exp Nephrol. 17 (2013) 751-764.

[31] Vukićević T, Schulz M, Faust D, Klussmann E. The Trafficking of the Water Channel Aquaporin-2 in Renal Principal Cells—a Potential Target for Pharmacological Intervention in Cardiovascular Diseases, Front Pharmacol. 7 (2016) 23.

[32] Bouley R, Lu HA, Nunes P, Da Silva N, McLaughlin M, Chen Y, Brown D. Calcitonin has a vasopressin-like effect on aquaporin-2 trafficking and urinary concentration, J Am Soc Nephrol. 22 (2011) 59-72.

[33] Yang T, Michele DE, Park J, Smart AM, Lin Z, Brosius FC, 3rd, Schnermann JB, Briggs JP. Expression of peroxisomal proliferator-activated receptors and retinoid X receptors in the kidney, Am J Physiol. 277 (1999) F966-973.

[34] Hong G, Lockhart A, Davis B, Rahmoune H, Baker S, Ye L, Thompson P, Shou Y, O'Shaughnessy K, Ronco P, et al. PPARgamma activation enhances cell surface ENaCalpha via up-regulation of SGK1 in human collecting duct cells, FASEB J. 17 (2003) 1966-1968.

[35] Xu J, Pan M, Wang X, Xu L, Li L, Xu C. Fluid Retention Caused by Rosiglitazone Is Related to Increases in AQP2 and αENaC Membrane Expression, PPAR Res. 2017 (2017) 8130968.

[36] Chen L, Yang B, McNulty JA, Clifton LG, Binz JG, Grimes AM, Strum JC, Harrington WW, Chen Z, Balon TW, et al. GI262570, a peroxisome proliferator-activated receptor {gamma} agonist, changes electrolytes and water reabsorption from the distal nephron in rats, J Pharmacol Exp Ther. 312 (2005) 718-725.

[37] Zhou L, Panasiuk A, Downton M, Zhao D, Yang B, Jia Z, Yang T. Systemic PPARgamma deletion causes severe disturbance in fluid homeostasis in mice, Physiol Genomics. 47 (2015) 541-547.

[38] Xiao-Yan Z, Bing W, You-Fei G. Nuclear Receptor Regulation of Aquaporin-2 in the Kidney, Int J Mol Sci. 17 (2016) 1105.

[39] Li N. Critical role of PPARγ in water balance, Physiol Genomics. 47 (2015) 538-540.

[40] Penna C, Tullio F, Femmino S, Rocca C, Angelone T, Cerra MC, Gallo MP, Gesmundo I, Fanciulli A, Brizzi MF, et al. Obestatin regulates cardiovascular function and promotes cardioprotection through the nitric oxide pathway, J Cell Mol Med. 21 (2017) 3670-3678.

[41] Su XJ, Dong RX, Li YP, Yang SG, Li ZF. Obestatin and cardiovascular health, Peptides. 52 (2014) 58-60.

[42] Tremblay F, Perreault M, Klaman LD, Tobin JF, Smith E, Gimeno RE. Normal food intake and body weight in mice lacking the G protein-coupled receptor GPR39, Endocrinology. 148 (2007) 501-506.

[43] Lauwers E, Landuyt B, Arckens L, Schoofs L, Luyten W. Obestatin does not activate orphan G protein-coupled receptor GPR39, Biochem Biophys Res Commun. 351 (2006) 21-25.

[44] Moechars D, Depoortere I, Moreaux B, de Smet B, Goris I, Hoskens L, Daneels G, Kass S, Ver Donck L, Peeters T, et al. Altered gastrointestinal and metabolic function in the GPR39-obestatin receptor-knockout mouse, Gastroenterology. 131 (2006) 1131-1141.

[45] Holst B, Egerod KL, Schild E, Vickers SP, Cheetham S, Gerlach LO, Storjohann L, Stidsen CE, Jones R, Beck-Sickinger AG, et al. GPR39 signaling is stimulated by zinc ions but not by obestatin, Endocrinology. 148 (2007) 13-20.

Appendix Tables:

<div align="center">Table A1. The primer sequences of the rat genes of interest studied</div>

Genes	Accession no.		Primer sequence（5′-3′）	Product size
Aqp2	NM_012909	For	TTGCAGGAACCAGACACTTG	217bp
		Rev	GCGGAGACGAGCACTTTTAC	
B-Actin	NM_031144	For	GTCAGGTCATCACTATCGGCAATG	147bp
		Rev	AGAGGTCTTTACGGATGTCAACG	

<div align="center">Table A2. The primer sequences of the mouse genes of interest studied</div>

Genes	Accession no.		Primer sequence（5′-3′）	Product size
Aqp1	NM_007472	For	AGGCTTCAATTACCCACTGGA	99bp
		Rev	CTTTGGGCCAGAGTAGCGAT	
Aqp2	NM_009699	For	ATGTGGGAACTCCGGTCCATA	137bp
		Rev	ACGGCAATCTGGAGCACAG	
Aqp3	NM_016689	For	CCTTGGCATCTTGGTGGCT	75bp
		Rev	AGGAAGCACATTGCGAAGGT	
Aqp4	NM_009700	For	ATCAGCATCGCTAAGTCCGTC	88bp
		Rev	GAGGTGTGACCAGGTAGAGGA	
B-Actin	NM_007393	For	GGCTGTATTCCCCTCCATCG	154bp
		Rev	CCAGTTGGTAACAATGCCATGT	
Pparg	NM_00127330	For	AGACCACTCGCATTCCTTTG	155bp
		Rev	TCGCACTTTGGTATTCTTGG	
V2r	NM_019404	For	TGACCGAGACCCGCTGTTA	111bp
		Rev	CGACCCCGTCGTATTAGGG	
Fgf23	NM_022657	For	ATGCTAGGGACCTGCCTTAGA	100bp
		Rev	AGCCAAGCAATGGGGAAGTG	
Myo1f	NM_053214	For	CTTTCACTGGCAGAGTCACAA	108bp
		Rev	ATGAAGCGTTTGCGGAGGTT	
Scnn1g	NM_011326	For	GCACCGACCATTAAGGACCTG	118bp
		Rev	GCGTGAACGCAATCCACAAC	
Slc8a1	NM_001112798	For	CTTCCCTGTTTGTGCTCCTGT	78bp
		Rev	AGAAGCCCTTTATGTGGCAGTA	
Ahr	NM_013464	For	AGCCGGTGCAGAAAACAGTAA	100bp
		Rev	AGGCGGTCTAACTCTGTGTTC	
Arid4b	NM_198122	For	ACTGAAGGTAGGAGCTATTGTGG	198bp

Gene	Accession		Primer	Size
		Rev	AGTGGGAGCTGGTCTAGTGTT	
Bco2	NM_133217	For	TGTCAAGGTTTGAGCCACCTA	195bp
		Rev	GGTCGTAATGAGGATGTGCAG	
Brca1	NM_009764	For	CGAATCTGAGTCCCCTAAAGAGC	89bp
		Rev	AAGCAACTTGACCTTGGGGTA	
Cebpg	NM_009884	For	AGCGGCTTACAGCAGGTTC	124bp
		Rev	GGCGGTATTCGTCACTATTCC	
Chac1	NM_026929	For	CTGTGGATTTTCGGGTACGG	122bp
		Rev	CCCCTATGGAAGGTGTCTCC	
Col1a2	NM_007743	For	GTAACTTCGTGCCTAGCAACA	230bp
		Rev	CCTTTGTCAGAATACTGAGCAGC	
Crebbp	NM_001025432	For	GGCTTCTCCGCGAATGACAA	136bp
		Rev	GTTTGGACGCAGCATCTGGA	
Creb1	NM_009952	For	AGCAGCTCATGCAACATCATC	152bp
		Rev	AGTCCTTACAGGAAGACTGAACT	
Creb3	NM_013497	For	AAGGCTCCGCTGGACTTAGA	170bp
		Rev	TGTGGAAGGGAGTAGTTGTGA	
Creb5	NM_172728	For	AGGATCTTCTGCCGTCTTGAT	152bp
		Rev	GCGCAGCCTTCAGTCTCAT	
Crebzf	NM_145151	For	CTGCCCGTCTTAATCGGCTC	155bp
		Rev	CCGTAGGTAGCGACTCTCCTC	
Cth	NM_145953	For	TTCCTGCCTAGTTTCCAGCAT	124bp
		Rev	GGAAGTCCTGCTTAAATGTGGTG	
Cux1	NM_009986	For	TGACCTGAGCGGTCCTTACA	85bp
		Rev	TGGGGCCATGCCATTTACATC	
Cyr61	NM_010516	For	CTGCGCTAAACAACTCAACGA	109bp
		Rev	GCAGATCCCTTTCAGAGCGG	
Cxcl12	NM_001012477	For	TGCATCAGTGACGGTAAACCA	146bp
		Rev	TTCTTCAGCCGTGCAACAATC	
Eif4g1	NM_001005331	For	AAGACCTCATCTCGCATCCG	143bp
		Rev	TGTTCTCGGTGCTCTTCCATC	
Insr	NM_010568	For	ATGGGCTTCGGGAGAGGAT	121bp
		Rev	GGATGTCCATACCAGGGCAC	
Nfatc1	NM_001164112	For	GACCCGGAGTTCGACTTCG	97bp
		Rev	TGACACTAGGGGACACATAACTG	

Gene	Accession		Primer sequence	Product size
Prkar2b	NM_011158	For	CCAGTAAGGGTGTCAACTTCG	179bp
		Rev	GGACTCTGCATCGTCTTCCTC	
Pten	NM_008960	For	TGGATTCGACTTAGACTTGACCT	180bp
		Rev	GCGGTGTCATAATGTCTCTCAG	
Smad4	NM_008540	For	ACACCAACAAGTAACGATGCC	83bp
		Rev	GCAAAGGTTTCACTTTCCCCA	
Tsc1	NM_022887	For	ATGGCCCAGTTAGCCAACATT	106bp
		Rev	CAGAATTGAGGGACTCCTTGAAG	
Dusp1	NM_013642	For	GTTGTTGGATTGTCGCTCCTT	129bp
		Rev	TTGGGCACGATATGCTCCAG	
Efna1	NM_010107	For	CCCGGAGAAGCTGTCTGAGA	177bp
		Rev	ACATGGGCCTGGGGATTATGA	
Enc1	NM_007930	For	CTGTTTCATAAGTCCTCCTACGC	169bp
		Rev	CACCACTGAACATGGCTTCG	
Eri2	NM_027698	For	GAGAAAGTCAGTTACACCAGCAA	96bp
		Rev	CAGGTAGACTCAAAGTCAACGAC	
Foxc1	NM_008592	For	CCCCGGACAAGAAGATCACTC	109bp
		Rev	AGGTTGTGCCGTATGCTGTTC	
Gadd45a	NM_007836	For	CCGAAAGGATGGACACGGTG	121bp
		Rev	TTATCGGGGTCTACGTTGAGC	
Gnaq	NM_008139	For	GGTCGGGCTACTCTGACGA	117bp
		Rev	ACTTGTATGGGATCTTGAGCGT	
Il1rap	NM_008364	For	TGCCTGGGGGAATTGTCAC	221bp
		Rev	CTTAGCCCGCTTCAGCTCTTT	
Mga	NM_013720	For	GAGGAGCACCTACCTTCTTTGT	89bp
		Rev	ACGGGCATCTCGATTAGTAACT	
Mllt10	NM_001252561	For	GTTGGGCTCATGTGGTTTGTG	79bp
		Rev	AAAACGATTGGCTCCATTGTAGA	
Mthfd2	NM_008638	For	AGTGCGAAATGAAGCCGTTG	149bp
		Rev	GACTGGCGGGATTGTCACC	
Nr2c2	NM_011630	For	GACTCTGCGGTAGCCTCAC	119bp
		Rev	AGGATGAACTGCTGTTTAGAGGA	
Nr4a2	NM_013613	For	GTGTTCAGGCGCAGTATGG	153bp
		Rev	TGGCAGTAATTTCAGTGTTGGT	
Ogt	NM_139144	For	GACGCAACCAAACTTTGCAGT	108bp

		Rev	TCAAGGGTGACAGCCTTTTCA	
Pdlim5	NM_001190857	For	TTCAACATGCCTCTGACAATCTC	80bp
		Rev	ACCACGTCCCTATTCTGACA	
Pikfyve	NM_011086	For	TCCCCGACACTGGACTCTG	208bp
		Rev	GGCTGGCCCAACTTGAACT	
Prdx6	NM_007453	For	CGCCAGAGTTTGCCAAGAG	115bp
		Rev	TCCGTGGGTGTTTCACCATTG	
Rabep1	NM_019400	For	CTTCGTTCTGTCGTGATGCC	277bp
		Rev	ACTGGTTGTGTTGTTGTCGTT	
Rin1	NM_145495	For	TATGACACACCTGATACCAGAGG	189bp
		Rev	AGTGTTAGATTTCCGCACCAG	
Rtp4	NM_023386	For	TGGGAGCAGACATTTCAAGAAC	179bp
		Rev	ACCTGAGCAGAGGTCCAACTT	
Steap1	NM_027399	For	GGTCGCCATTACCCTCTTGG	188bp
		Rev	GGTATGAGAGACTGTAAACAGCG	
Steap2	NM_028734	For	ATGGGAAGCCCTAAGAGCCT	126bp
		Rev	AAGCCGAATGGTCAGAGACTT	
Tcf4	NM_013685	For	CGAAAAGTTCCTCCGGGTTTG	196bp
		Rev	CGTAGCCGGGCTGATTCAT	
Tmx1	NM_028339	For	CACTTGGGGCGTCTTATGGTT	111bp
		Rev	CCAGTTCTCATCGGTGAGGAC	
Pde4b	18578	For	CGCAGGGAGTCGTTCCTCTA	263bp
		Rev	CTCCTGTGGTCGCACACTTG	
Rgs2	NM_009061	For	GAGAAAATGAAGCGGACACTCT	197bp
		Rev	GCAGCCAGCCCATATTTACTG	
Sgk1	NM_001161849	For	CTGCTCGAAGCACCCTTACC	175bp
		Rev	TCCTGAGGATGGGACATTTTCA	
Sorl1	NM_011436	For	AGCAGGAGGGAGTCGAGAC	170bp
		Rev	GTTCCTAGCCGGAGATCGC	
Vldlr	NM_013703	For	GAGTCTGACTTCGTGTGCAAA	83bp
		Rev	GAACCGTCTTCGCAATCAGGA	
Klhl30	NM_027551	For	CATCTGCCTTCACATGCCCAA	206bp
		Rev	ACGTCTCGCAGTTCCACAC	
Chd9	NM_177224	For	GAGGGCAGTTTGATTGGACAA	178bp
		Rev	CGTTCCTCTGTGATTGGTTGAAT	

Slc26a1	NM_178743	For	AGTGTATGCGGGAACACATGC	141bp
		Rev	CGAAGGCGTAAGCAATCAGAG	
Fam46c	NM_001142952	For	AACTGGGATCAGGTTAGCCG	212bp
		Rev	CAACCCAAGCCGTTGTCTT	
Vwce	NM_027913	For	GCCTACATCTTGATCCCGTTG	234bp
		Rev	GGAACAGACATTGGGAGCGA	
Scn8a	NM_011323	For	CCCGACAGTTTCAAGCCTTTC	240bp
		Rev	CGTCAAATAGTACGGGTCAAAGT	
Zc3h7b	NM_001081016	For	GGCAGCCTGCTACTTCACC	98bp
		Rev	GGAACAGTGCCCGGATACT	
Nrg4	NM_032002	For	CACGCTGCGAAGAGGTTTTTC	104bp
		Rev	CGCGATGGTAAGAGTGAGGA	
FOXP4	NM_001110824	For	GCTGTTACTGCTACCTCGTTT	107bp
		Rev	CTGTCTCTCCGAGATGTGAGC	